Acousto-optic bistability with fluctuations

M. F. Wehner
Fusion Engineering Program, Nuclear Engineering Department, University of Wisconsin, Madison, Wisconsin 53706

J. Chrostowski
Division of Electrical Engineering, National Research Council of Canada, Ottawa, Canada K1A 0R6

W. J. Mielniczuk
Division of Chemistry, National Research Council of Canada, Ottawa, Canada K1A 0R6
(Received 12 January 1984)

A newly developed numerical method of solving nonlinear Fokker-Planck equations is applied to study an acousto-optic bistability with additive noise. The time evolution of the probability distribution for the transmitted light is calculated for a double-well potential. The time-dependent moments are calculated.

I. INTRODUCTION

The nonlinear effect of optical bistability is currently under extensive investigation in a variety of different materials and systems.[1] This attention stems mainly from the broad application of such systems in integrated optics and telecommunication. In addition, a bistable system is of theoretical interest as an example of an open system driven to a stationary nonequilibrium state by an external source. Bistable behavior has been observed in a number of intrinsic all-optical interferometers—GaAs, InSb, CdS platelets, and several hybrid optic-electronic elements. Recently a new type of hybrid bistability has been proposed by Chrostowski and Delisle.[2] Among other characteristics, self-pulsing and bifurcations to chaos have been observed.[3]

The purpose of our paper is to study the role of noise on the time evolution of the acousto-optic bistability. A great deal of previous attention has focused on solving different aspects of the nonlinear bistable equations augmented by the addition of noise to account for the fluctuations in the system.[4] Part of this work attacks the much more general problem of macroscopic systems far from a thermodynamic equilibrium state. Many of these systems, including optical ones, can be described by the nonlinear Fokker-Planck equation.[5–7] In recent years a major effort has been devoted to deriving a formal solution of the nonlinear Fokker-Planck equation in terms of a path integral. Wehner and Wolfer[8] have recently presented a new, very efficient numerical method based on the path sum. We present an improved version of this algorithm and use it to calculate the time evolution of the probability distribution of output light intensity in the acousto-optic bistable system in several cases. Then the mean light intensity $\langle I\rangle\sim\langle q\rangle$ and time-dependent variance $\langle I\rangle^2-\langle I^2\rangle$ are calculated using the above probability distribution.

In Sec. II the acousto-optic bistability is briefly described. In Sec. III the Fokker-Planck equation is discussed and in Sec. IV the numerical method of Wehner and Wolfer is outlined. Section V describes the results.

II. ACOUSTO-OPTIC BISTABILITY

Figure 1 shows a schematic diagram of the experimental layout of Chrostowski *et al.*[2,3] If the delay in the feedback loop is small compared with the other time constants in the system, the time evolution can be described by the equation

$$\tau\frac{dq}{dt}=\beta K I_L T(q-B)-(q-\beta U_0)\,, \tag{1}$$

where the voltage q is proportional to the transmitted light intensity, β is the gain in the feedback amplifier, K is a geometrical factor which includes the sensitivity of the detector (V/W), I_L is the laser intensity, $-1\le B\le 1$ is a constant controlled by the rf biasing, U_0 is the bias voltage, and τ is the lumped time constant in the loop. The nonlinear transmission $T(x)$ for the Bragg-type acousto-optic interaction can be written as $T(x)=\sin^2[(\pi/2)x]$ with saturation for $x>1$, and where the voltage at the input of the rf driver is proportional to the square root of the acoustic power within the crystal.

The steady-state solutions of Eq. (1) and experiment show bistability and hysteresis in three modes of operation: input laser intensity, feedback gain, and bias voltage

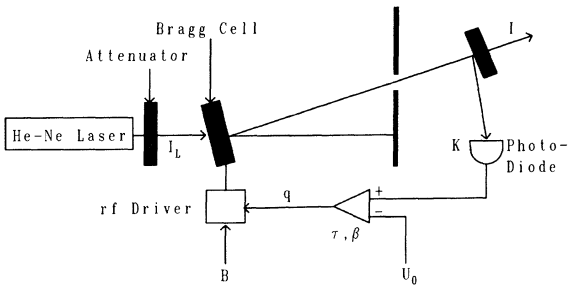

FIG. 1. Acousto-optic bistability of Ref. 2.

tuning. For the present purpose we restrict our analysis to bias voltage tuning.

In this experiment the deterministic behavior governed by Eq. (1) is influenced by at least two sources of noise: electrical and/or laser intensity fluctuations. We will simulate them by adding a white noise source to Eq. (1).

The Langevin equation, the stochastic equivalent of Eq. (1), reads

$$\dot{q}=k(q)+F(t)\ , \tag{2}$$

where $\dot{q}=\tau dq/dt$ and the nonlinear drift or force function is

$$k(q)=\begin{cases} A\beta\sin^2[(\pi/2)(q-B)]-(q-\beta U_0), & |q-B|\le 1 \\ A\beta-(q-\beta U_0), & |q-B|>1 \end{cases} \tag{3}$$

$$A=KI_L\ .$$

The random force $F(t)$ is assumed to be a real Gaussian random process with zero mean and an autocorrelation function of the form

$$\langle F(t)F(t')\rangle=Q\delta(t-t')\ . \tag{4}$$

Similar one- or two-dimensional Langevin equations have appeared in other physical realizations of optical bistability.[4] If information is needed only about certain properties of the system such as statistical moments, the Langevin equation can be solved by Monte Carlo techniques. This involves generating a sufficiently large number of trajectories, evaluating the functional form for each, and then appropriately averaging the moments. To obtain a full description of the stochastic evolution of the system, the Fokker-Planck solution is needed.

III. FOKKER-PLANCK EQUATION

The Langevin equation (2) is linear in the fluctuating force, hence the stochastically equivalent Fokker-Planck equation can readily be written by following the prescription of Stratonovich.[9] The evolution of the probability distribution $P(q,t)$ which describes both the deterministic path as determined by the drift function (3) as well as fluctuations away from this path as defined by the diffusion constant Q, is given by

$$\frac{\partial P(q,t)}{\partial t}=-\frac{\partial}{\partial q}[k(q)P(q,t)]+\tfrac{1}{2}Q\frac{\partial^2}{\partial q^2}P(q,t)\ . \tag{5}$$

Even in the case of constant diffusion, Eq. (5) calls for numerical analysis since it is exactly or approximately solvable only for specific forms of the drift function $k(q)$. The potential $W(q)$ corresponding to the drift function (3) is defined as

$$W(q)=-\int_{-\infty}^{q} dq'\,k(q')\ . \tag{6}$$

Depending on the choice of parameters it can have one or two or more minima—the latter cases leading to bistability or multistability.

Figure 2 shows the deterministic characteristics of acousto-optic bistability with the experimentally sound parameters $A=2.03$, $B=0$, $U_0=-0.5473$, $\beta=1$. It shows three possible steady states: metastable q_3, unstable q_2, and stable q_1 indicated by the zeros of the drift function and the extreme of the potential function. In an experiment only the stable states q_1 and q_3 can be observed yielding a hysteresis curve when one of the parameters is varied back and forth. In Fig. 2(c) the zeros of the drift function are plotted as a function of the bias voltage U_0 for fixed A, β, and β_0 to illustrate how the bistability can be switched on and off by varying such an external parameter.

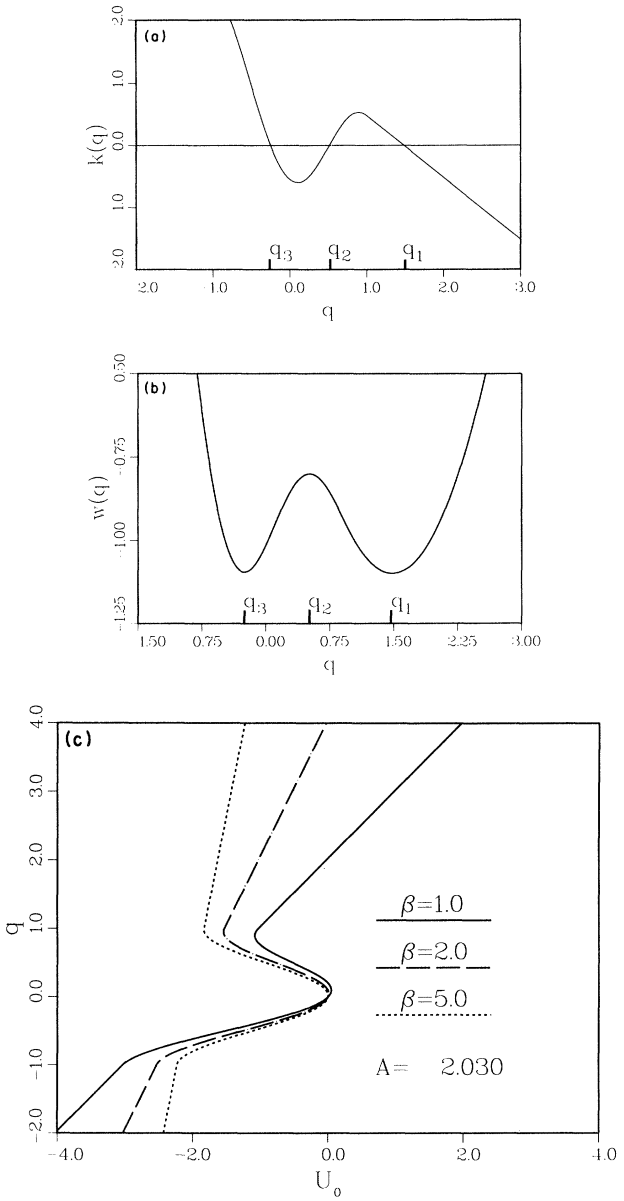

FIG. 2. (a) $k(q)$ is plotted vs q for the values $A=2.03$, $\beta=1$, and $U_0=-0.5473$. Note the three zeros: q_3, metastable; q_2, unstable; and q_1, stable. (b) The potential $W(q)$ corresponding to the drift function in (a) is shown as a function of q. (c) The zeros of $k(q)$ are plotted vs U_0 for the values $A=2.03$ and $\beta=1.0,2.0,5.0$.

The stationary solution of Eq. (5) can be written as

$$P_{\text{stat}}(q)=C\exp\left[-\frac{2}{Q}W(q)\right]\ , \tag{7}$$

where the normalization constant $1/C = \int_{-\infty}^{+\infty} P_{\text{stat}}(q')dq'$ and $W(q)$ is given by

$$W(q)=\begin{cases}\dfrac{q^2}{2}-\beta q(U_0+A), & q<B-1\\ \dfrac{q^2}{2}+\dfrac{A\beta}{2\pi}\sin[\pi(q-B)]-\beta q\left[U_0+\dfrac{A}{2}\right] & \\ \quad -(B-1)\dfrac{A\beta}{2}, & B-1\le q\le B+1\\ \dfrac{q^2}{2}-\beta q(U_0+A)+\beta A, & q>B+1.\end{cases} \tag{8}$$

The long-time evolution of the probability density $P(q,t)$ in the case when initially the system was in the state given by $P(q,t=0)=\delta(q-q_0)$ can be represented in the form[9]

$$P(q,t)=P_{\text{stat}}(q)+\sum_{\substack{n=2\\ \lambda_n\neq 0}}^{\infty}\frac{u_n(q)u_n(q_0)}{P_{\text{stat}}(q)}\exp(-\lambda_n t)\,, \tag{9}$$

where $u_n(q)$ $(n=2,3,\ldots)$ denote the eigenfunctions of the following eigenproblem:

$$\frac{d}{dq}[k(q)u_n(q)]-\tfrac{1}{2}Q\frac{d^2}{dq^2}u_n(q)=\lambda_n u_n(q)\,, \tag{10}$$

with $u_n(q)\to 0$ for $q\to\pm\infty$.

Let us assume that the eigenvalues of Eq. (10) are ordered in such a way that $\lambda_2<\lambda_3<\lambda_4<\cdots$. Then for times $t>10/\lambda_2$ all but the first two terms on the right-hand side of Eq. (9) may neglected, resulting in

$$P(q,t)\approx P_{\text{stat}}(q)+u_2(q)u_2(q_0)\frac{1}{P_{\text{stat}}(q)}\exp(-\lambda_2 t)\,. \tag{11}$$

It is possible to give an explicit analytical form for the eigenvalue λ_2 in the case when

$$\frac{W(q_3)-W(q_2)}{Q/2}\gg 1\,. \tag{12}$$

Namely,[10,11]

$$\lambda_2\simeq\frac{\sqrt{|W''(q_3)|\,|W''(q_2)|}}{2\pi}\exp\left[-\frac{2}{Q}[W(q_2)-W(q_3)]\right]. \tag{13}$$

Here, W'' denotes the second derivative of the potential $W(q)$. The explicit form of the eigenfunction $u_2(q)$ in the general case was given by Matkowsky and Schuss.[7]

The mean first-passage time or mean escape time T_2, the time scale of diffusion from an initial state located in the vicinity of the metastable state q_3, to a final state near the stable state q_1, is related to λ_2 by[6]

$$T_2=1/\lambda_2\,. \tag{14}$$

For $Q=0.05$, $A=2.03$, $B=0$, $\beta=1.0$, and $U_0=-0.5473$ (as in Fig. 2), we find that $\lambda_2=0.476\times 10^{-5}$, hence $T_2=2\times 10^5$. Hence the time required for the probability distribution to converge to the steady state is very long. This reflects the relative "stiffness" of the Fokker-Planck equation. As will be seen in Sec. IV, due to requirements of the numerical method, the computer time required to fully investigate this case would be prohibitively long. However, by simply increasing the noise by a factor of 2, i.e., $Q=0.1$ and keeping all other parameters unchanged, the mean first-passage time is reduced to $T_2=580$. This case is easily handled by the requirements of the numerical techniques. It should be noted that the unit of time is dimensionless and is converted to real time through multiplication by 0.5 μsec.

IV. DETAILS OF THE NUMERICAL PATH-SUM SOLUTION TO NONLINEAR FOKKER-PLANCK EQUATIONS

The nonlinear Fokker-Planck equation possesses a formal solution in terms of a Feynman or path integral.[12–17] Wehner and Wolfer[8] have developed an iterative numerical technique to evaluate this type of functional integral based upon its discrete equivalent, the path sum. In this previous work the probability distribution function was represented as a histogram composed solely of vertical and horizontal elements. In the next higher-order representation a linear relationship between the points of the probability distribution is specified. Hence, the resulting figure is composed of a series of trapezoidal rather than rectangular elements.

The path sum for the one-dimensional nonlinear Fokker-Planck equation under natural boundary conditions is given as

$$P(q,t+\tau)=\int_{-\infty}^{+\infty}dq_0\,G(q,q_0,\tau)P(q_0,t)\,. \tag{15}$$

The short time propagator $G(q,q_0,\tau)$ must satisfy the Fokker-Planck equation to order $O(\tau^2)$, and hence can take on a variety of forms. The simplest form, given by Dekker,[12] is

$$G(q,q_0,\tau)=\frac{1}{\sqrt{2\pi Q(q_0)\tau}}\exp\left[-\frac{[q-q_0-k(q_0)\tau]^2}{2Q(q_0)\tau}\right]. \tag{16}$$

The trapezoidal representation of the probability-distribution function is defined as

$$P(q,t)=\frac{(q-q_i)}{(q_{i+1}-q_i)}P_{i+1}(t)+\frac{(q_{i+1}-q)}{(q_{i+1}-q_i)}P_i(t)\,,\qquad q_i\le q\le q_{i+1} \tag{17}$$

where the q axis has been subdivided into a discrete grid network. Putting Eq. (17) into Eq. (15), integrating dq over the interval $q_i\le q\le q_{i+1}$, and dividing the integral over dq_0 in the same manner as the grid, the following relationships between the nodal points result:

$$P_i(t+\tau)+P_{i+1}(t+\tau)=\sum_{j=1}^{N}[P_j(t)A_{ij}(\tau)+P_{j+1}(t)B_{ij}(\tau)]\,, \tag{18}$$

where

$$A_{ij}=\frac{2}{\Delta q_i\,\Delta q_j}\int_{q_i}^{q_{i+1}}dq\int_{q_j}^{q_{j+1}}dq'G(q,q',\tau)(q_{j+1}-q')$$

and (19)

$$B_{ij}=\frac{2}{\Delta q_i\,\Delta q_j}\int_{q_i}^{q_{i+1}}dq\int_{q_j}^{q_{j+1}}dq'G(q,q',\tau)(q'-q_j)\ .$$

This set of equations may be evaluated iteratively. The main requirements for the numerical solution to approach the exact results are[8] (a) the grid must be subdivided such that

$$\Delta q_i=q_{i+1}-q_i=[2Q(q_i)\tau]^{1/2}\ .$$

(b) The time step must be chosen to satisfy $\tau<Q(q)/[k(q)]^2$ over all values of q where $P(q,t)$ has an appreciable value. (c) The grid must be constructed such that all values of q where $P(q,t)$ has an appreciable value lie within the grid.

The distribution function is further subject to the normalization condition

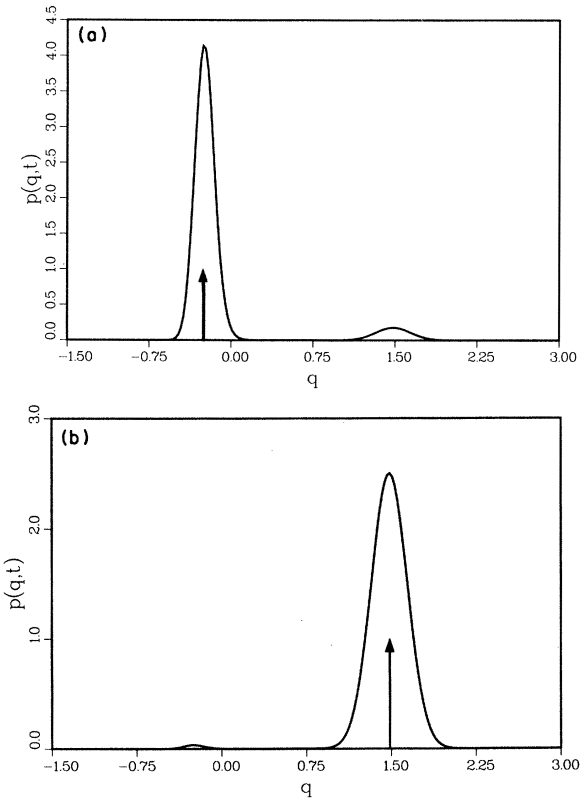

FIG. 3. (a) Numerical calculation of the distribution function $P(q,t)$ subject to the initial condition $P(q,t=0)=\delta(q-q_0)$ is shown at the time $t=10000$. q_0 is chosen as -0.2577 which is near the metastable state. The values $Q=0.05$, $A=2.03$, $\beta=1.0$, and $U_0=-0.5473$ were used. The time step τ was chosen as 0.01 and the number of grid points N was 350. (b) The same as (a) except $q_0=1.48643$ which is near the stable point.

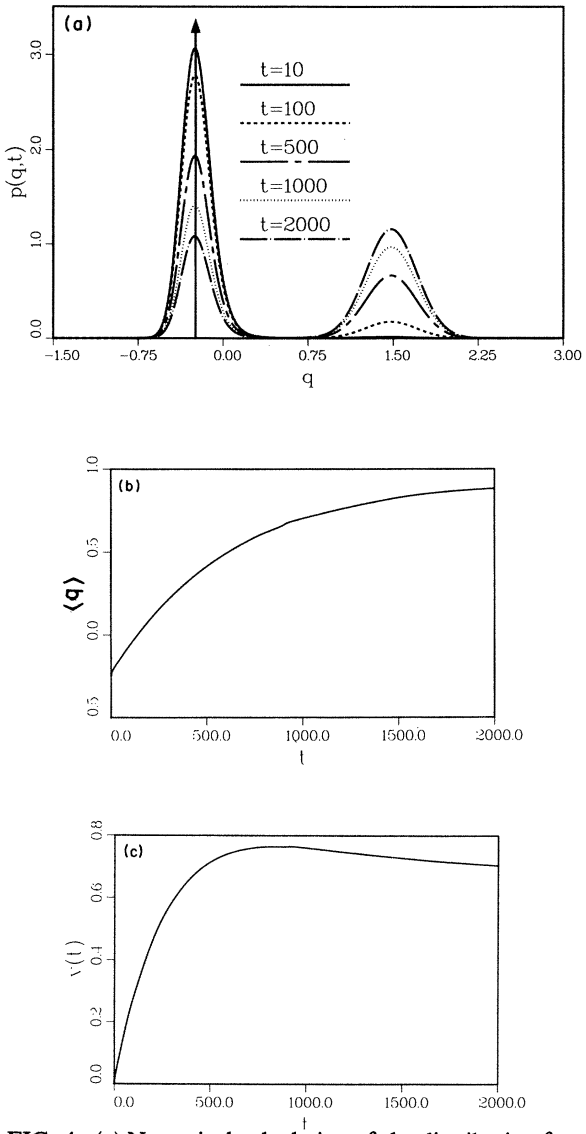

FIG. 4. (a) Numerical calculation of the distribution function $P(q,t)$ subject to the initial condition $P(q,t=0)=\delta(q-q_0)$ at various times. The values $Q=0.1$, $q_0=-0.24285$, $A=2.03$, $\beta=1.0$, and $U_0=-0.5473$ were used. Also, $\tau=0.01$ and $N=300$. At $t=2000$, the steady-state solution has been reached. (b) The mean value $\langle q\rangle$ of the system described by (a) as a function of time. (c) The variance $\langle q^2\rangle-\langle q\rangle^2$ of the system described by (a) as a function of time.

$$\sum_{i=1}^{N}\frac{(P_i+P_{i+1})}{2}\Delta q_i=1 \qquad (20)$$

after every iteration. Comparison between numerical and exact results for problems possessing analytical solutions typically reveals a factor of 10 improvement in the relative error using the trapezoidal representation as compared to the histogram representation.

Finally the mean value and the variance are defined as $m(t)=\langle q\rangle$ and $v(t)=\langle q^2\rangle-\langle q\rangle^2$, respectively, where $\langle q\rangle=\int_{-\infty}^{+\infty}qP(q,t)dq$ and $\langle q^2\rangle=\int_{-\infty}^{+\infty}q^2P(q,t)dq$. In

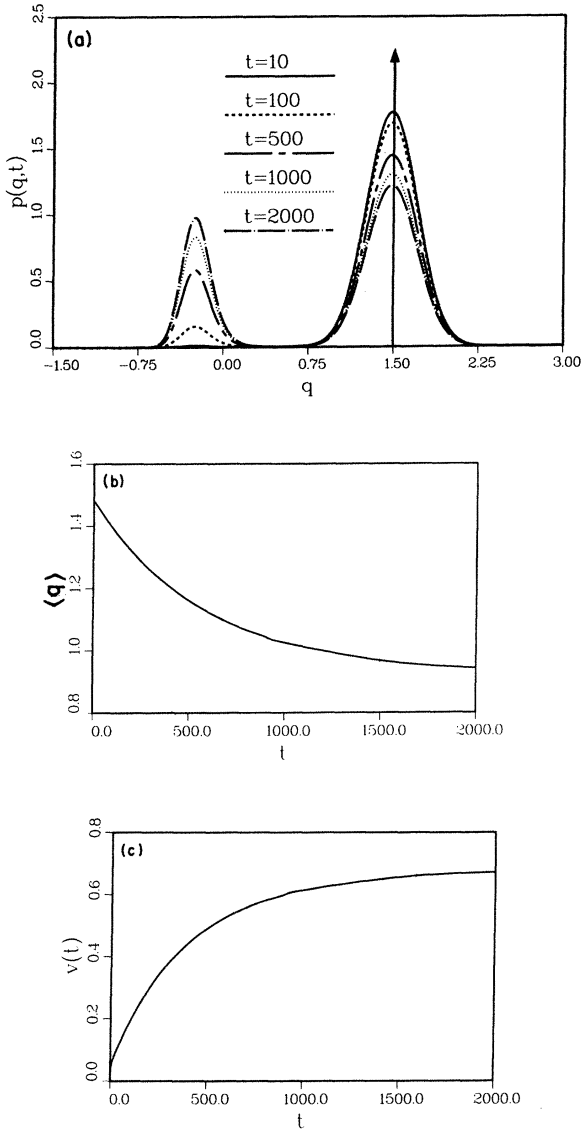

FIG. 5. (a) Same as Fig. 4(a) except $q_0=1.4864$. (b) The mean value $\langle q \rangle$ of the system described by (a) as a function of time. (c) The variance $\langle q^2 \rangle - \langle q \rangle^2$ of the system described by (a) as a function of time.

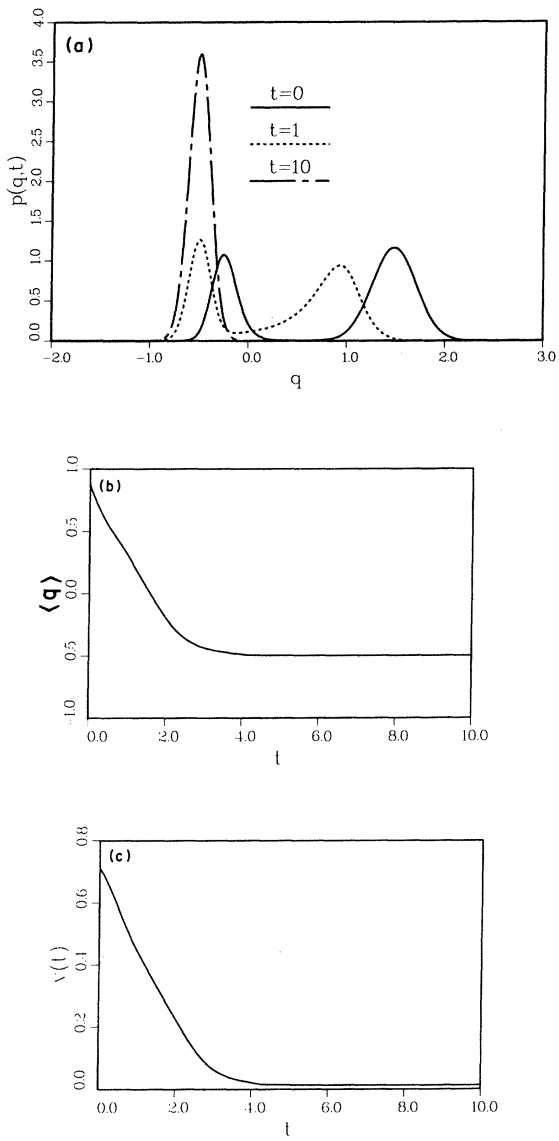

FIG. 6. (a) Numerical calculation of the distribution function $P(q,t)$ at various times subject to the steady-state solution $P(q, t=\infty)$ for the values $Q=0.1$, $A=2.03$, $\beta=1.0$, and $U_0=-0.5473$. At time $t=0$ the value of U_0 is perturbed to $U_0=-1.515$. As is evident from Fig. 2(c), this destroys the bistability. By the time $t=10.0$ the distribution function has reached the steady state. (b) The mean value $\langle q \rangle$ of the system described by (a) as a function of time. (c) The variance $\langle q^2 \rangle - \langle q \rangle^2$ of the system described by (a) as a function of time.

the trapezoidal representation these averages are approximated by the algorithm

$$\int_{-\infty}^{+\infty} f(q)P(q,t)dq = \frac{1}{2}\sum_{i=1}^{N}[f(q_i)P_i(t)+f(q_{i+1})P_{i+1}(t)]\Delta q_i \ . \quad (21)$$

V. RESULTS

Probability distributions for various values of the external parameters and at various times were calculated. In Fig. 3(a) the distribution function at time $t=10\,000$ for a very stiff system is shown. In this figure the initial condition is a delta function near the metastable point. As is evident, fluctuations drive this system toward bistability but as mentioned before, the time required to approach the steady state is significantly longer than this. Figure 3(b) shows the same system with an initial condition near the stable point. This configuration crosses the potential barrier of Fig. 2(b) considerably slower than that of Fig. 3(a) due to the slightly lower depth of the potential well.

In Fig. 4(a) the distribution function at various times is shown for a system characterized by the same drift func-

tion, potential well, and initial condition of Fig. 3(a) but subject to increased fluctuations. The mean escape time for this system was given before as $T_2 = 580$. However, a somewhat greater time than T_2 is required for the system to fully approach the steady state as illustrated by the distribution function itself and by plots of the experimentally measurable quantities, the mean and variance [Figs. 4(b) and 4(c), respectively]. In Figs. 5(a)–5(c), the same system as in Fig. 4 was solved subject to an initial condition in the vicinity of the stable point.

To investigate the effect of bias voltage switching, this same system is allowed to reach the steady state. Then, at $t=0$ the bias voltage U_0 is perturbed from -0.5473 to -1.515. As can be seen from Fig. 2(c), the system is no longer in the bistable regime. The numerical time evolution, shown in Figs. 6(a)–6(c), reveals that the time scale for the bistability to be destroyed is much shorter than that required for it to develop.

VI. CONCLUSIONS

The effects of additive noise on a recently proposed acousto-optic bistability model have been studied numerically. The numerical technique utilized is based on the formal path-integral solution of the Fokker-Planck equation. Various initial conditions leading to either an approach to or a degradation of a bistable configuration were investigated revealing vastly different time scales for these two phenomena. Time scales are also greatly influenced by the relative magnitude of the fluctuations.

ACKNOWLEDGMENTS

We would like to thank Dr. T. Balaban and Dr. W. G. Wolfer for their useful insights. This work was supported by the National Research Council of Canada and by the U.S. Department of Energy under Contract No. DE-AC02-82ER50282.

[1]See, e.g., *Optical Bistability,* edited by C. Bowden, M. Ciftan, and H. R. Robl (Plenum, New York, 1981); *Coherence and Quantum Optics V,* edited by L. Mandel and E. Wolf (Plenum, New York, in press).

[2]J. Chrostowski and C. Delisle, Opt. Commun. 41, 71 (1982).

[3]J. Chrostowski, Phys. Rev. A 26, 3023 (1982); J. Chrostowski, R. Vallee, and C. Delisle, Can. J. Phys. 61, 1143 (1983).

[4]G. A. Agarwal, L. M. Narducci, R. Gilmore, and D. H. Feng, Phys. Rev. A 19, 620 (1978); R. Bonifacio, M. Gronchi, and L. A. Lugiato, *ibid.* 18, 2266 (1978); A. Zardecki, *ibid.* 23, 1281 (1980); P. D. Drummond, K. J. McNeil, and D. F. Walls, *ibid.* 22, 1672 (1980); J. Chrostowski, A. Zardecki, and C. Delisle, *ibid.* 24, 345 (1981); H. E. Schmidt, S. W. Koch, and H. Haug, Z. Phys. B 51, 85 (1983).

[5]A. Schenzle and H. Brand, Phys. Rev. A 20, 1628 (1979).

[6]R. Gilmore, Phys. Rev. A 20, 2510 (1979).

[7]B. J. Matkowsky and Z. Schuss, SIAM J. Appl. Math. 40, 242 (1981).

[8]M. F. Wehner and W. G. Wolfer, Phys. Rev. A 27, 2663 (1983).

[9]R. L. Stratonovich, *Topics in the Theory of Random Noise* (Gordon and Breach, New York, 1963).

[10]H. A. Kramers, Physica (Utrecht) 7, 284 (1940).

[11]N. G. van Kampen, *Stochastic Processes in Physics and Chemistry* (North-Holland, Amsterdam 1981).

[12]H. Dekker, Physica (Utrecht) 85A, 363 (1976).

[13]H. Haken, Z. Phys. B 24, 321 (1976).

[14]R. Graham, Z. Phys. B 26, 281 (1976).

[15]H. Dekker, Phys. Rev. A 19, 2102 (1979).

[16]C. Wissel, Z. Phys. B 35, 185 (1979).

[17]H. Grabert and M. S. Green, Phys. Rev. A 19, 1747 (1979).